Estimating Instrument Spectral Response Functions Using Sparse Representations and Quadratic Envelopes

Jihanne El Haouari [1,2], Marcus Carlsson[3], Jean-Yves Tourneret[1,2], Herwig Wendt[2], Jean-Michel Gaucel [4] and Christelle Pittet[5]

[1] TéSA Laboratory, Toulouse, France.
[2] IRIT-ENSEEIHT, CNRS, University of Toulouse, Toulouse, France.
[3] Department of Mathematics Lund University, Sweden
[4] Thales Alenia Space Cannes, France
[5] Centre National d'Etudes Spatiales, Centre Spatial de Toulouse, France

Abstract—**The estimation of high resolution spectrometer Instrument Spectral Response Functions (ISRFs) is crucial because an imperfect knowledge of these functions can induce errors in the measurements. The state-of-the-art for this problem currently relies on the use of parametric models, which frequently lack flexibility to accurately model real-world ISRFs. To address this limitation, this paper proposes and investigates the use of sparse representations for modeling and estimating ISRFs, where the ISRFs are decomposed in a fixed dictionary of atoms. To estimate the sparse coefficient vector, a novel sparsity inducing regularization of the problem based on quadratic envelopes is studied and compared to the classical LASSO estimator and to a greedy method based on the Orthogonal Matching Pursuit (OMP) algorithm. Results for simulated ISRFs from the MicroCarb mission indicate that the proposed spectral representations yield excellent ISRF estimates, and that the use of quadratic envelopes can yield significantly better precision than competing methods.**

Index Terms—**Instrument Spectral Response Function (ISRF), Sparse representations, quadratic envelope regularization, LASSO, Orthogonal Matching Pursuit (OMP).**

I. INTRODUCTION

Context and related work. Models based on sparse representations have been extensively used in several applications such as image denoising, classification or restoration [1]–[3]. This paper studies the potential interest of these models for estimating the Instrument Spectral Response Functions (ISRFs) of a spectrometer. The measured spectrum of a spectrometer at a given wavelength λ_l, denoted as $s(\lambda_l)$, is obtained by a convolution between the ISRF at wavelength λ_l denoted as I_l and a high resolution theoretical spectrum s_{th} [4], [5], i.e.,

$$s(\lambda_l) = \sum_{n=-N/2}^{N/2} s_{\text{th}}(\lambda_l - n\Delta)I_l(n\Delta) + \epsilon_l, \qquad (1)$$

where Δ is the sampling period used for the $N+1$ points of the ISRF wavelength grid, λ_l is a wavelength usually not defined in the same grid (i.e., $\lambda_l \neq k\Delta, k \in \mathbb{N}$) and ϵ_l is the Gaussian noise for the lth measurement. The ISRF estimation problem has previously been conducted by using parametric models such as Gaussian or generalized Gaussian models, which constitute the state-of-the-art for ISRF estimation [6]. However, these models can be of limited accuracy under the operational conditions of realworld missions. As an example, for the MicroCarb mission currently investigated by the Centre National d'Etudes Spatiales (CNES) in Toulouse, France [7], the accuracy expected to determine CO_2 concentrations necessitates a precise knowledge of the ISRFs at the considered wavelengths with relative errors less than 1%. This threshold is not always guaranteed by parametric models [8], attesting the importance of finding new methods for ISRF estimation.

Goals, contributions and outline. The objective of this work is to overcome the previously mentioned limitations concerning ISRF estimation by modeling ISRFs using sparse representations, as proposed in [9], and to translate this approximation to formulate an inverse problem for (1) (cf. Section II). The main contribution of this work consists in evaluating the performance of a quadratic envelope-based regularization to solve the sparse representation problem with a predefined number of atoms (cf. Section III). The proposed method is compared with classical sparse representation methods such as LASSO and the greedy OMP method. Section IV presents experiments on simulated data generated by the CNES for the MicroCarb mission. The results indicate that the proposed approach yields excellent ISRF estimates and that the quadratic envelope based-regularization often leads to significantly better precision than the use of ℓ_1 or ℓ_0 penalties. Conclusions and future works are described in Section V.

II. SPARSE REPRESENTATION FOR ISRFs

A. Problem formulation

Each ISRF I_l of a spectrometer depends on its central wavelength λ_l. Thus, the ISRF problem resulting from (1) implies to estimate, for each wavelength λ_l, the corresponding response function by using one measurement $s(\lambda_l)$. In order to solve this ill-posed problem, we assume that the ISRFs do not vary much in a small observation window around the wavelength λ_l of interest $\mathcal{W}_l = \left\{ \lambda_{l-\frac{L}{2}}, ..., \lambda_{l+\frac{L}{2}} \right\}$. In vectorial form, (1) can be rewritten as follows:

$$s_l = S_{\text{th},l} I_l + \epsilon_l, \qquad (2)$$

where $\epsilon_l \in \mathbb{R}^{L+1}$ is a noise vector and

$$s_l \triangleq [s(\lambda_{l-\frac{L}{2}}), ..., s(\lambda_{l+\frac{L}{2}})] \in \mathbb{R}^{L+1},$$
$$S_{\text{th},l} \triangleq [S_{\text{th}}(\lambda_{l'} - n\Delta)]_{\substack{l-\frac{L}{2} \leq l' \leq l+\frac{L}{2} \\ -\frac{N}{2} \leq n \leq \frac{N}{2}}} \in \mathbb{R}^{(L+1) \times (N+1)},$$
$$I_l \triangleq [I_l(-N\Delta/2), ..., I_l(N\Delta/2)] \in \mathbb{R}^{N+1}.$$

The ISRF estimation problem then reduces to finding the vector I_l that minimizes the residual error $||s_l - S_{\text{th},l} I_l||_2^2$.

B. ISRF model using a sparse approximation

We model the ISRF I_l as a linear combination of a small number K of atoms belonging to a dictionary $\Phi \in \mathbb{R}^{(N+1) \times N_{\text{dict}}}$ composed of N_{dict} atoms, i.e.,

$$I_l \approx I_l^K = \Phi \alpha_l, \qquad (3)$$

where $I_l^K \in \mathbb{R}^{N+1}$ is the approximation of the ISRF I_l obtained using K atoms, and $\alpha_l = (\alpha_{l,1}, ..., \alpha_{l,N_{\text{dict}}})^T \in \mathbb{R}^{N_{\text{dict}}}$ is a sparse

vector with K non-zero coefficients. This representation can easily be translated to the inverse problem (1). Indeed, the convolution between the theoretical spectrum and the ISRF can be written using the sparse decomposition (3) so that the measured spectrum is also decomposed with the same coefficient vector $\boldsymbol{\alpha}_l$, i.e.,

$$s_l \approx \boldsymbol{S}_{\text{th},l} \boldsymbol{I}_l^K = \boldsymbol{\Psi}_l \, \boldsymbol{\alpha}_l, \tag{4}$$

with a new dictionary $\boldsymbol{\Psi}_l \triangleq \boldsymbol{S}_{\text{th},l} \boldsymbol{\Phi} \in \mathbb{R}^{(L+1) \times N_{\text{dict}}}$. The dictionary $\boldsymbol{\Phi}$ and the theoretical spectra $\boldsymbol{S}_{\text{th},l}$ being known, $\boldsymbol{\Psi}_l$ is also a known dictionary. Thus, estimating the ISRF from the measured spectrum reduces to finding a sparse coefficient vector $\boldsymbol{\alpha}_l$ yielding a good approximation of s_l in (4).

C. Resolution methods

The sparse representation problem (4) can be mathematically formulated in different ways [1]. One way is to use an l_0 pseudo-norm penalty $|| \cdot ||_0$ with penalty parameter μ:

$$\arg \min_{\boldsymbol{\alpha}_l} L(\boldsymbol{\alpha}_l, \mu) = \arg \min_{\boldsymbol{\alpha}_l} ||s_l - \boldsymbol{\Psi}_l \boldsymbol{\alpha}_l||_2^2 + \mu ||\boldsymbol{\alpha}_l||_0. \tag{5}$$

This problem is non convex and NP-hard, and therefore can be solved using many approximations and heuristics. A first family of approaches uses greedy algorithms, e.g., based on Matching Pursuit (MP) or Orthogonal Matching Pursuit (OMP). These algorithms have been widely used to solve (5) and have shown good performance in many applications [10], [11]. The main drawback of greedy algorithms is that they are heuristic and hence not connected with the minimization of any particular functional. A second approach consists in replacing the l_0 penalty term in (5) with another regularization leading to a simpler optimization problem. A standard approach is the LASSO regularization, which replaces the l_0 pseudo-norm penalty with a convex l_1 norm [12]. The main drawback of the LASSO algorithm is that it comes along with a well known shrinking bias, especially for large values of μ needed to find very sparse solutions, i.e., with a low number of atoms K. As shown in our experiments, OMP gives the best results for small values of K for the application considered in this work. Thus, LASSO tends to perform worse for the whole range of hyperparameters μ (since low values of μ give representations with a lot of atoms and high values of μ introduce a shrinking bias that must be corrected once the atoms are selected).

Recently, a more flexible family of regularizations based on quadratic envelopes has been introduced [13]. The quadratic envelope can be applied to the indicator function of a predetermined amount of non-zero coefficients K, and ideally the minimization of this functional (in combination with a data-fidelity term) gives sparse representations with K non-zero terms without introducing a shrinking bias [14]. This method is presented in more detail in the following section.

III. QUADRATIC ENVELOPES

A. Introduction to quadratic envelopes

The reason for using $\mu ||\boldsymbol{\alpha}_l||_1$ in the LASSO method as a proxy for $\mu ||\boldsymbol{\alpha}_l||_0$ in (5) is that the function $\boldsymbol{\alpha}_l \mapsto \mu ||\boldsymbol{\alpha}_l||_0$ is highly discontinuous and non-convex, particularly near the sought optimum. Indeed, for every vector $\boldsymbol{\alpha}_l$ whose components are all non-zero, the function is constantly equal to N, whereas for near sparse vectors $\boldsymbol{\alpha}_l$ with $||\boldsymbol{\alpha}_l||_0 = K$, there are points taking any value in the range $\{K, \ldots, N\}$ arbitrarily close to $\boldsymbol{\alpha}_l$. On the other hand, the function $\boldsymbol{\alpha}_l \mapsto ||\boldsymbol{\alpha}_l||_1$ is convex and continuous, making the corresponding proximal operator easily computable and suitable to popular algorithms such as the alternating direction method of

multipliers (ADMM) [15] and the forward-backward splitting (FBS) method (see [16] and references therein). However, as mentioned earlier, it is known that this introduces a shrinking bias and thus a degraded solution.

If we ignore the computational difficulty of solving (5), another drawback of both (5) and ℓ_1-minimization is that they contain a hyperparameter μ which needs to be tuned to find a certain number of atoms. If we are looking for a predefined number of, say K, non-zero atoms, one could replace $\mu ||\boldsymbol{\alpha}_l||_0$ with the (parameter-free) penalty ι_K, i.e., the indicator functional of K-sparse vectors $\{\boldsymbol{\alpha}_l : ||\boldsymbol{\alpha}_l||_0 \le K\}$. Of course, minimizing the resulting functional is also NP-hard and therefore not feasible in practice. Quadratic envelopes were introduced to overcome the above mentioned draw-backs. Just like the convex envelope, the quadratic envelope is not a penalty in itself, but a method that can regularize any ill-behaved penalty. Since we observed good results for OMP with low values of K in previous work [9], we investigate here to replace $\mu ||\boldsymbol{\alpha}_l||_0$ in (5) with the quadratic envelope of the indicator functional ι_K. On the downside, the resulting cost functional is non-convex and there is no guarantee that the found minimum, using either ADMM or FBS, is the global minimizer or that it is indeed K-sparse. On the other hand, it was proved in [14] that the cost functional in question often has a unique local minimizer (hence also global minimizer) that coincides with the so called "oracle solution", i.e., the best solution obtained for a known support (which is the best solution that one can expect). Moreover, it was observed numerically that the solution obtained using either FBS or ADMM initialized at 0 or randomly indeed tends to be the oracle solution (which is K-sparse).

In general, given a regularization parameter $\gamma > 0$ and a functional $f : \mathbb{R}^N \to \mathbb{R}$, the quadratic envelope $\mathcal{Q}_\gamma(f)$ is defined as the pointwise supremum of all quadratic functions of the form $\boldsymbol{\alpha}_l \mapsto r - \frac{\gamma}{2} ||\boldsymbol{\alpha}_l - \boldsymbol{\beta}||^2$ that are below f, where the supremum is taken over all $r \in \mathbb{R}$ and $\boldsymbol{\beta} \in \mathbb{R}^N$. In [13], it was shown that, given certain conditions, regularizing with the quadratic envelope gives a new continuous penalty that has the same global minimizer as the original, i.e.,

$$\mathcal{Q}_\gamma(f)(\boldsymbol{\alpha}_l) + ||s_l - \boldsymbol{\Psi}_l \boldsymbol{\alpha}_l||_2^2 \tag{6}$$

has the same global minimizer as the corresponding problem with $\mathcal{Q}_\gamma(f)$ replaced by f.

For illustration purpose, Figure 1 displays the different regularizers $||\boldsymbol{x}||_1$, $\mathcal{Q}_2(||\boldsymbol{x}||_0)$ and $\mathcal{Q}_2(\iota_1)$ in the first quadrant of $\mathbb{R}^2$. As is clear to see, l_1 has a linearly growing penalty also for 1-sparse points, i.e., points along either axis, which is the cause of the aforementioned shrinking bias. The quadratic envelope applied to the l_0-penalty for this particular illustration, shown in the middle, turns out to be the same as the MCP-penalty from [17]. This envelope has a bias also for 1-sparse vectors, which stops to grow at ± 1 and thus removes the bias from larger non-zero coordinates in the sought minimizer. However, this has a large plateau in the square $\min(|x_1|, |x_2|) > 1$, and is hence prone to get stuck around non-sparse local minima. The penalty $\mathcal{Q}_2(\iota_1)$ on the other hand looks a bit like the l_1-penalty away from the axes while still ensuring that $\mathcal{Q}_2(\boldsymbol{x}) = 0$ for any 1-sparse $\boldsymbol{x}$, thus merging the benefits of both previous candidates.

The application of the quadratic envelope to the particular penalty ι_K in various frameworks has been extensively studied theoretically (see, e.g., [14], [18]–[20]) and it has been shown to give consistently superior results than competing methods. In this paper we evaluate its performance for the sparse ISRF problem. In order to minimize (6) using FBS or ADMM, one should compute the proximal operator of $\mathcal{Q}_\gamma(f)$. Recall that the proximal operator of $||\boldsymbol{\alpha}_l||_1$ is the soft
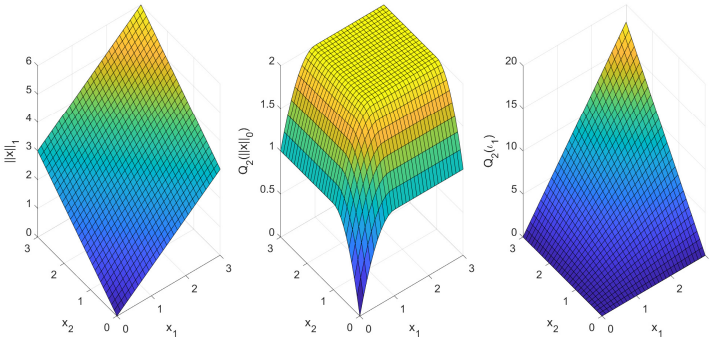
Fig. 1. Illustration of the different regularizations in 2D; $||x||_1$, $\mathcal{Q}_2(||x||_0)$ and $\mathcal{Q}_2(\iota_1)$.

thresholding operator, which is separable (i.e., acts on each coordinate independently of adjacent values) and very simple to implement. This reflects the fact that the l_1-penalty is also separable. The penalty $\mathcal{Q}_2(\iota_K)$ is much more intricate and is not separable, so that the value of each particular coordinate in the proximal operator depends on all other values in the input vector. How to compute this proximal operator goes beyond the scope of this paper but the details can be found in [21] or in the readme-file of https://github.com/Marcus-Carlsson/Quadratic-Envelopes, where the proximal operator in question also can be downloaded.

B. Proposed algorithm

In this article, the quadratic envelope-based approach was implemented using the FISTA algorithm [22], as described in [21]. Therein, a regularization parameter $0 < \gamma < ||\Psi_l||^2$ needs to be fixed [13]: we found that if this parameter is too small, the method hardly manages to converge and remains close to the least square solution, and that a suitable value for this parameter is $\gamma = \frac{||\Psi_l||^2}{1.2}$, which is consistent with the conjecture outlined in the technical implementation part of reference [14]. For this algorithm, we use $T = 10000$ iterations with a "stepsize" parameter in the proximal operator set to $\rho = \frac{||\Psi_l||^2}{0.9}$, close to its lower theoretical bound, see [14] for details. Finally, multiple values of the cardinality K are tested. Note that with these choices, no further hyperparameter tuning is needed for the quadratic envelope, in contrast to LASSO. A more precise description of the algorithm based on the quadratic envelope for the ISRF estimation is made in Algorithm 1 for each λ_l.

Algorithm 1 Quadratic envelope algorithm for estimating ISRFs.

Input: Measured spectrum s_l, Dictionary Ψ_l, Desired cardinality K, Regularization parameters γ and ρ, Number of iterations T

Output: ISRF estimation $\hat{I}_l^{(T)}$

1: Initialize $\hat{I}_l^{(0)}$;
2: $\hat{I}_{l,\text{resp}}^{(1)} = 0$;
3: **for** $1 \leq t \leq T$: **do**
                     ▷ Use of FISTA acceleration process:
4:     $\tilde{I}_l^{(t)} = \hat{I}_l^{(t-1)} + \frac{t-1}{t+2}\left(\hat{I}_l^{(t-1)} - \hat{I}_{l,\text{resp}}^{(1)}\right)$;
5:     $\hat{I}_{l,\text{resp}}^{(t)} = \hat{I}_l^{(t-1)}$;
                    ▷ Compute proximal operator:
6:     $\hat{I}_l^{(t)} = \text{ProxQgammaiota}\left(\tilde{I}_l^{(t)} - \frac{1}{\rho}\Psi_l^T(\Psi_l\tilde{I}_l^{(t)} - s_l), K, \gamma, \rho\right)$;
7: **end for**

IV. NUMERICAL EXPERIMENTS

A. Datasets and simulation

Data. The data used in this paper results from simulations carried out by the CNES for the MicroCarb mission. The main objective of this mission is to monitor carbon dioxide fluxes at the Earth's surface and determine as accurately as possible the concentration of carbon dioxide in the atmosphere. The MicroCarb instrument is a spectrometer with high spectral resolution acquiring data in two infrared absorption bands (B2: $1.596 - 1.618\mu m$ and B3: $2.023 - 2.051\mu m$) to recover CO_2 absorption lines, and in two near-infrared bands (B1:$0.758 - 0.769\mu m$ and B4: $1.264 - 1.282\mu m$) to measure oxygen concentration. We present here results from the first band (B1). Similar results have been obtained for the other bands and are not reported here for space reasons. The theoretical spectrum used in the experiments was obtained using a radiative transfer software named 4A/OP [23]. The ISRFs and measured spectra were then obtained using a simulator of the MicroCarb instrument developed by CNES.

Dictionary, sparse representation and experimental setup. The dictionary Φ is built using the N_{dict} singular vectors associated with the largest singular values from a singular value decomposition (SVD) of examples of ISRFs, simulated for the chosen band. The size of the dictionary is $N_{\text{dict}}= 50$, and the values of K are chosen in the set $\{2, ..., 5\}$. The size of the observation window is $L= 40$. The noise is zero mean Gaussian and the signal to noise ratio (SNR) is set to 55dB. The performance is evaluated in terms of residual error for the measured spectrum s and normalized absolute error for the ISRF approximation (at a given wavelength), i.e.,

$$\text{E}_l = \sum_{n=1}^{N+1} |I_l[n] - \hat{I}_l[n]| / \sum_{n=1}^{N+1} I_l[n]. \qquad (7)$$

LASSO and OMP Algorithms. The LASSO algorithm was implemented using the MATLAB LASSO function that uses a penalty with parameter $\mu > 0$ leading to a shrinking bias [24]. Thus we re-estimate the value of the non-zero coefficients by using least squares after convergence. In order to set the parameter μ, the LASSO MATLAB function was run over a range of different values and the value of μ yielding the desired cardinality K was selected.

B. Results

Comparison for fixed cardinality. Figure 2 displays the results obtained with $K = 3$ atoms in terms of spectrum reconstruction (top), residual error (center) and ISRF approximation error (bottom) for all 1024 wavelengths in the first band B1. These results lead to the following observations. First, the LASSO estimator consistently behaves poorly compared to the other methods, both in terms of residual error (and thus in capacity to find a sparse coefficient vector that leads to high fidelity with the measurements), and in terms of approximation quality for the ISRF. Note that the LASSO solution does not satisfy the constraint of having relative errors less than 1% demanded for the MicroCarb mission. Second, OMP leads to overall better results, in particular in terms of ISRF approximation error, with relative errors less than 1%. Third, and most importantly, the quadratic envelope approach succeeds in many cases to find a significantly better solution to the sparse representation problem and also leads to significantly better results for ISRF approximation.
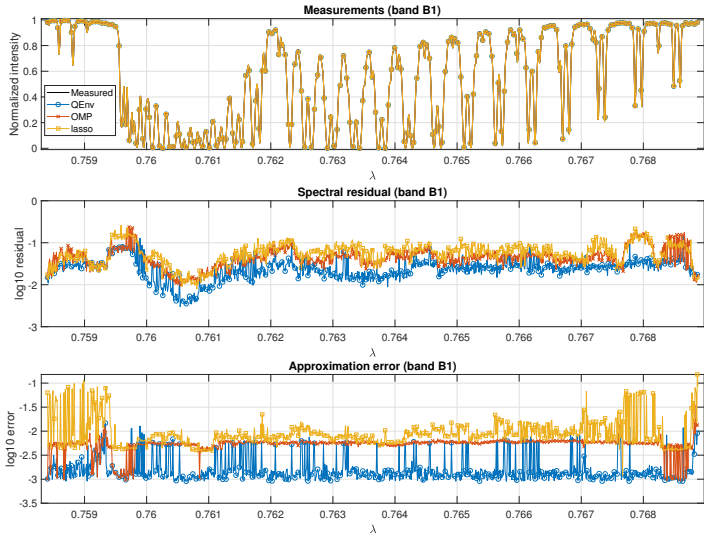
Fig. 2. Reconstructions, residual errors and ISRF approximation errors of the measured spectra using sparse representations via quadratic envelope, OMP or LASSO ($K = 3$).
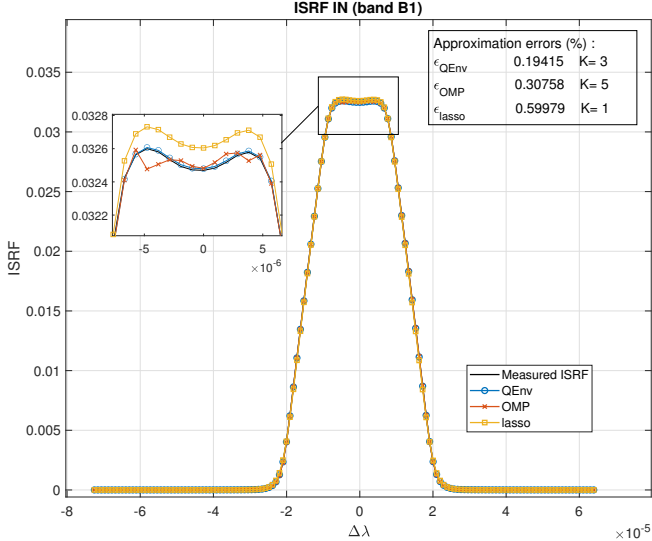
TABLE I
MEAN RESIDUAL AND APPROXIMATION ERRORS FOR DIFFERENT SNRS AND DIFFERENT METHODS (QENV, OMP AND LASSO).

$\times 10^{-3}$		residual error			ISRF approximation error		
SNR		$K = 3$	$K = 4$	$K = 5$	$K = 3$	$K = 4$	$K = 5$
40 dB	QEnv	573.1	550.1	532.2	4.3	8.4	12.4
	OMP	580.1	538.5	510.1	7.3	9.6	13.9
	LASSO	588.2	554.5	528.0	24.6	35.6	49.0
55 dB	QEnv	27.4	25.8	23.1	1.9	2.9	3.5
	OMP	49.6	26.6	21.2	5.5	3.3	3.1
	LASSO	60.6	43.2	33.2	11.9	14.6	18.6
80 dB	QEnv	9.5	8.7	6.7	1.7	2.3	2.3
	OMP	33.6	9.2	4.6	5.4	2.6	1.9
	LASSO	48.6	30.9	19.6	10.9	13.0	15.9

TABLE II
MEAN COMPUTATION TIME FOR ESTIMATING ONE ISRF USING THE DIFFERENT METHODS (QENV, OMP AND LASSO).

$\times 10^{-2}$		QEnv	OMP	LASSO
Computation time (s)		24.07	0.325	3.73

Fig. 3. Examples of ISRF approximations using a sparse representation via quadratic envelope, OMP or LASSO (K chosen for each method as the value that provide the most accurate approximation of the ISRF).

Examples of estimated ISRFs. Figure 3 shows the results of the approximation problem for one arbitrarily chosen ISRF using for each method the value of K yielding the best solution. Clearly, the quadratic envelope approach (QEnv) best fits the shape of the ISRF, further corroborating the conclusions from the previous paragraph.

Choice of cardinality. Table I reports residual errors and approximation errors for several values for K. We observe that increasing K systematically leads to a decrease in residual error, which is expected since the extra flexibility of using more atoms should allow the algorithms to improve the fit to the measurements. However, this does not necessarily lead to improved approximations for the ISRF. Indeed, the best ISRF average approximation results

are obtained for $K = 3$ for the quadratic envelope but for $K = 5$ for OMP. Interestingly, the results obtained with quadratic envelopes are consistently and significantly better that those obtained with OMP. This indicates that the former approach is effective in finding a good solution (even with a smaller number of atoms) and that adding further atoms fits the noise in the data.

Robustness to noise. Table I provides results obtained for different noise levels, including the SNR value of 55dB expected for the MicroCarb mission. Both the residual error and the approximation error are smaller for larger values of SNR, as expected. Note that the reduction in residual error is significantly larger than the reduction of approximation error when the SNR is increased: this indicates that the sparse approach is effective in finding a good approximation for the ISRF, which is little affected by the noise, and that the spectral residual is essentially given by the noise.

To conclude, these results suggest that the proposed sparse representation is an interesting strategy for the estimation of ISRFs from spectral measurements, also in the presence of noise. Moreover, the use of quadratic envelopes leads to a very promising performance, at the price of an increased computation time (see Table II) when compared to the greedy OMP approach.

V. CONCLUSION

This paper proposed a new method to solve the Instrument Spectral Response Function (ISRF) estimation problem from spectral measurements. This method relies on a regularization of a sparse problem using a quadratic envelope. Simulation results showed that for some configuration, this approach manages to find better ISRF estimates when compared to LASSO or OMP algorithms, at the price of an increased computation cost. Future work will take into account some physical effects such as stray light, as they can degrade the estimation of ISRFs for specific wavelengths. Using dictionary learning methods, such as those based on the K-SVD algorithm, can also be considered to analyze the importance of the dictionary selection.

REFERENCES

[1] Z. Zhang, Y. Xu, J. Yang, X. Li, and D. Zhang, "A survey of sparse representation: Algorithms and applications," *IEEE Access*, vol. 3, pp. 490–530, 2015.

[2] K. Schnass and P. Vandergheynst, "Dictionary preconditioning for greedy algorithms," *IEEE Trans. Signal Process.*, vol. 56, no. 5, pp. 1994–2002, 2008.

[3] M. A. T. Figueiredo, R. D. Nowak, and S. J. Wright, "Gradient projection for sparse reconstruction: Application to compressed sensing and other inverse problems," *IEEE J. Sel. Topics Signal Process.*, vol. 1, no. 4, pp. 586–597, 2007.

[4] K. Sun, X. Liu, G. Huang, G. González Abad, Z. Cai, K. Chance, and K. Yang, "Deriving the slit functions from OMI solar observations and its implications for ozone-profile retrieval," *Atmos. Meas. Tech.*, vol. 10, no. 10, pp. 3677–3695, 2017.

[5] M. Hamidouche and G. Lichtenberg, "In-flight retrieval of SCIA-MACHY instrument spectral response function," *Remote Sens.*, vol. 10, no. 3, pp. 401, 2018.

[6] S. Beirle, J. Lampel, C. Lerot, H. Sihler, and T. Wagner, "Parameterizing the instrumental spectral response function and its changes by a super-gaussian and its derivatives," *Atmos. Meas. Tech.*, vol. 10, no. 2, pp. 581–598, 2017.

[7] E. Cansot, L. Pistre, M. Castelnau, P. Landiech, L. Georges, Y. Gaere-mynck, and P. Bernard, "MicroCarb instrument, overview and first results," *Proc. SPIE 12777, Inf. Conf. Space Optics*, vol. 12777, no. 1277734, pp. 1–13, 2022.

[8] J. El Haouari, J.-Y. Tourneret, H. Wendt, C. Pittet, and J.-M. Gaucel, "Approximation et estimation de reponses spectrales d'instruments," in *XXIXeme Colloque sur le traitement du signal et des images*, Grenoble, 2023, number 2023-1081, pp. p. 85–88, GRETSI - Groupe de Recherche en Traitement du Signal et des Images.

[9] J. El Haouari, J.-M. Gaucel, C. Pittet, J.-Y. Tourneret, and H. Wendt, "Estimation of instrument spectral response functions using sparse representations in a dictionary," in *IEEE Int. Geosci. Remote Sens. Symp. (IGARSS 2024)*, Athens, Greece, July 2024, to be published.

[10] S. G. Mallat and Z. Zhang, "Matching pursuits with time-frequency dictionaries," *IEEE Trans. Signal Process.*, vol. 41, no. 12, pp. 3397–3415, 1993.

[11] Y. C. Pati, R. Rezaiifar, and P. S. Krishnaprasad, "Orthogonal matching pursuit: recursive function approximation with applications to wavelet decomposition," in *Proc. Asilomar Conf. Signals, Systems and Computers*, Pacific Grove, CA, USA, Nov. 1-3 1993, pp. 40–44.

[12] R. Tibshirani, "Regression shrinkage and selection via the lasso," *J. R. Stat. Soc. Ser. B Methodol.*, vol. 58, pp. 267–288, 1996.

[13] M. Carlsson, "On convex envelopes and regularization of non-convex functionals without moving global minima," *J. Optim. Theory Appl.*, vol. 183, no. 1, pp. 66–84, 2019.

[14] M. Carlsson, D. Gerosa, and C. Olsson, "An unbiased approach to compressed sensing," *Inverse Probl.*, vol. 36, no. 11, pp. 115014, Oct. 2020.

[15] S. Boyd, N. Parikh, E. Chu, B. Peleato, and J. Eckstein, "Distributed optimization and statistical learning via the alternating direction method of multipliers," *Found. Trends Mach. Learn.*, vol. 3, pp. 1–122, 2011.

[16] P. L. Combettes, J.-C. Pesquet, H. H. Bauschke, R. S. Burachik, V. Elser, D. R. Luke, and H. Wolkowicz, *Proximal Splitting Methods in Signal Processing*, Springer, New York, 2011.

[17] C.-H. Zhang, "Nearly unbiased variable selection under minimax concave penalty," *Ann. Stat.*, vol. 38, no. 2, pp. 894–942, 2010.

[18] M. Carlsson, D. Gerosa, and C. Olsson, "An unbiased approach to low rank recovery," *SIAM J. Optim.*, vol. 32, no. 4, pp. 2969–2996, 2022.

[19] D. Gerosa, M. Carlsson, and C. Olsson, "Bias versus non-convexity in compressed sensing," *J. Math. Imaging Vis.*, vol. 64, no. 4, pp. 379–394, 2022.

[20] J. Bacca, M. Carlsson, B. Monroy, and H. Arguello, "Plug-and-play algorithm coupled with low-rank quadratic envelope regularization for compressive spectral imaging," in *ICASSP 2024-2024 IEEE International Conference on Acoustics, Speech and Signal Processing (ICASSP)*. IEEE, 2024, pp. 2505–2509.

[21] M. Carlsson and D. Gerosa, "On phase retrieval via matrix completion and the estimation of low rank PSD matrices," *Inverse Probl.*, vol. 36, no. 1, pp. 015006, Dec. 2019.

[22] A. Beck and M. Teboulle, "A fast iterative shrinkage-thresholding algorithm for linear inverse problems," *SIAM J. Imaging Sci.*, vol. 2, no. 1, pp. 183–202, 2009.

[23] NOVELTIS, CNES, and LMD, "4A/OP - operational release for 4A - automatized atmospheric absorption atlas," https://4aop.noveltis.fr/references-and-publications.

[24] C.-H. Zhang and J. Huang, "The sparsity and bias of the Lasso selection in high-dimensional linear regression," *Ann. Stat.*, vol. 36, no. 4, pp. 1567 – 1594, 2008.